JACOBIAN ADVERSARIALLY REGULARIZED NETWORKS FOR ROBUSTNESS

Anonymous authors
Paper under double-blind review

ABSTRACT

Adversarial examples are crafted with imperceptible perturbations with the intent to fool neural networks. Against such attacks, adversarial training and its variants stand as the strongest defense to date. Previous studies have pointed out that robust models that have undergone adversarial training tend to produce more salient and interpretable Jacobian matrices than their non-robust counterparts. A natural question is whether a model trained with an objective to produce salient Jacobian can result in better robustness. This paper answers this question with affirmative empirical results. We propose Jacobian Adversarially Regularized Networks (JARN) as a method to optimize the saliency of a classifier's Jacobian by adversarially regularizing the model's Jacobian to resemble natural training images. Image classifiers trained with JARN show improved robust accuracy compared to standard models on the MNIST, SVHN and CIFAR-10 datasets, uncovering a new angle to boost robustness without using adversarial training.

1 INTRODUCTION

Deep learning models have shown impressive performance in a myriad of classification tasks (LeCun et al., 2015). Despite their success, deep neural image classifiers are found to be easily fooled by visually imperceptible adversarial perturbations (Szegedy et al., 2013). These perturbations can be crafted to reduce accuracy during test time or veer predictions towards a target class. This vulnerability not only poses a security risk in using neural networks in critical applications like autonomous driving (Bojarski et al., 2016) but also presents an interesting research problem about how these models work.

Many adversarial attacks have come into the scene (Carlini & Wagner, 2017; Papernot et al., 2018; Croce & Hein, 2019), not without defenses proposed to counter them (Gowal et al., 2018; Zhang et al., 2019). Among them, the best defenses are based on *adversarial training* (AT) where models are trained on adversarial examples to better classify adversarial examples during test time (Madry et al., 2017). While several effective defenses that employ adversarial examples have emerged (Qin et al., 2019; Shafahi et al., 2019), generating strong adversarial training examples adds non-trivial computational burden on the training process (Kannan et al., 2018; Xie et al., 2019).

Adversarially trained models gain robustness but are also observed to produce more salient Jacobian matrices (Jacobians) at the input layer as a side effect (Tsipras et al., 2018). These Jacobians visually resemble their corresponding images for robust models but look much noisier for standard non-robust models. It is shown in theory that the saliency in Jacobian is a result of robustness (Etmann et al., 2019). A natural question to ask is this: can an improvement in Jacobian saliency induce robustness in models? In other words, could this side effect be a new avenue to boost model robustness? To the best of our knowledge, this paper is the first to show affirmative findings for this question.

To enhance the saliency of Jacobians, we draw inspirations from neural generative networks (Choi et al., 2018; Dai & Wipf, 2019). More specifically, in generative adversarial networks (GANs) (Goodfellow et al., 2014), a generator network learns to generate natural-looking images with a training objective to fool a discriminator network. In our proposed approach, Jacobian Adversarially Regularized Networks (JARN), the classifier learns to produce salient Jacobians with a regularization objective to fool a discriminator network into classifying them as input images. This method offers a new way to look at improving robustness without relying on adversarial examples during

training. With JARN, we show that directly training for salient Jacobians can advance model robustness against adversarial examples in the MNIST, SVHN and CIFAR-10 image dataset. When augmented with adversarial training, JARN can provide additive robustness to models thus attaining competitive results. All in all, the prime contributions of this paper are as follows:

- We show that directly improving the saliency of classifiers' input Jacobian matrices can increase its adversarial robustness.
- To achieve this, we propose Jacobian adversarially regularized networks (JARN) as a method to train classifiers to produce salient Jacobians that resemble input images.
- Through experiments in MNIST, SVHN and CIFAR-10, we find that JARN boosts adversarial robustness in image classifiers and provides additive robustness to adversarial training.

2 Background and Related Work

Given an input $\mathbf{x}$, a classifier $f(\mathbf{x};\theta) : \mathbf{x} \mapsto \mathbb{R}^k$ maps it to output probabilities for k classes in set C, where θ is the classifier's parameters and $\mathbf{y} \in \mathbb{R}^k$ is the one-hot label for the input. With a training dataset D, the standard method to train a classifier f is empirical risk minimization (ERM), through $\min_\theta \mathbb{E}_{(\mathbf{x},\mathbf{y})\sim D}\mathcal{L}(\mathbf{x},\mathbf{y})$, where $\mathcal{L}(\mathbf{x},\mathbf{y})$ is the standard cross-entropy loss function defined as

$$\mathcal{L}(\mathbf{x},\mathbf{y}) = \mathbb{E}_{(\mathbf{x},\mathbf{y})\sim D}\left[-\mathbf{y}^\top \log f(\mathbf{x})\right] \tag{1}$$

While ERM trains neural networks that perform well on holdout test data, their accuracy drops drastically in the face of adversarial test examples. With an adversarial perturbation of magnitude ε at input $\mathbf{x}$, a model is robust against this attack if

$$\arg\max_{i\in C} f_i(\mathbf{x};\theta) = \arg\max_{i\in C} f_i(\mathbf{x}+\delta;\theta)\ , \quad \forall \delta \in B_p(\varepsilon) = \delta : \|\delta\|_p \leq \varepsilon \tag{2}$$

We focus on $p = \infty$ in this paper.

Adversarial Training To improve models' robustness, adversarial training (AT) (Goodfellow et al., 2016) seek to match the training data distribution with the adversarial test distribution by training classifiers on adversarial examples. Specifically, AT minimizes the loss function:

$$\mathcal{L}(\mathbf{x},\mathbf{y}) = \mathbb{E}_{(\mathbf{x},\mathbf{y})\sim D}\left[\max_{\delta\in B(\varepsilon)} \mathcal{L}(\mathbf{x}+\delta,\mathbf{y})\right] \tag{3}$$

where the inner maximization, $\max_{\delta\in B(\varepsilon)} \mathcal{L}(\mathbf{x}+\delta,\mathbf{y})$, is usually performed with an iterative gradient-based optimization. Projected gradient descent (PGD) is one such strong defense which performs the following gradient step iteratively:

$$\delta \leftarrow \mathrm{Proj}\left[\delta - \eta\ \mathrm{sign}\left(\nabla_\delta \mathcal{L}(\mathbf{x}+\delta,\mathbf{y})\right)\right] \tag{4}$$

where $\mathrm{Proj}(\mathbf{x}) = \arg\min_{\zeta\in B(\varepsilon)} \|\mathbf{x}-\zeta\|$. The computational cost of solving Equation (3) is dominated by the inner maximization problem of generating adversarial training examples. A naive way to mitigate the computational cost involved is to reduce the number gradient descent iterations but that would result in weaker adversarial training examples. A consequence of this is that the models are unable to resist stronger adversarial examples that are generated with more gradient steps, due to a phenomenon called obfuscated gradients (Carlini & Wagner, 2017; Uesato et al., 2018).

Since the introduction of AT, a line of work has emerged that also boosts robustness with adversarial training examples. Capturing the trade-off between natural and adversarial errors, TRADES (Zhang et al., 2019) encourages the decision boundary to be smooth by adding a regularization term to reduce the difference between the prediction of natural and adversarial examples. Qin et al. (2019) seeks to smoothen the loss landscape through local linearization by minimizing the difference between the real and linearly estimated loss value of adversarial examples. To improve adversarial training, Zhang & Wang (2019) generates adversarial examples by feature scattering, i.e., maximizing feature matching distance between the examples and clean samples.

Tsipras et al. (2018) observes that adversarially trained models display an interesting phenomenon: they produce salient Jacobian matrices ($\nabla_{\mathbf{x}}\mathcal{L}$) that loosely resemble input images while less robust standard models have noisier Jacobian. Etmann et al. (2019) explains that linearized robustness (distance from samples to decision boundary) increases as the alignment between the Jacobian and input image grows. They show that this connection is strictly true for linear models but weakens for non-linear neural networks. While these two papers show that robustly trained models result in salient Jacobian matrices, our paper aims to investigate whether directly training to generate salient Jacobian matrices can result in robust models.

Non-Adversarial Training Regularization Provable defenses are first proposed to bound minimum adversarial perturbation for certain type of neural networks (Hein & Andriushchenko, 2017; Raghunathan et al., 2018). One of the most advanced defense from this class of work (Wong et al., 2018) uses a dual network to bound the adversarial perturbation with linear programming. The authors then optimize this bound during training to boost adversarial robustness. Apart from this category, closer to our work, Jakubovitz & Giryes (2018) proposes a regularization term to reduce the Jacobian's Frobenius norm to decrease the effect input perturbations have on the model prediction. With a similar goal, Ross & Doshi-Velez (2018) shows that reducing the Frobenius norm of the input Hessian matrix improves adversarial robustness. Different from them, we train the classifier with an adversarial loss term to make the Jacobian resemble input images more closely.

3 JACOBIAN ADVERSARIALLY REGULARIZED NETWORKS (JARN)

Motivation Robustly trained models are observed to produce salient Jacobian matrices that resemble the input images. This begs a question in the reverse direction: will an objective function that encourages Jacobian to more closely resemble input images, will standard networks become robust? To study this, we look at neural generative networks where models are trained to produce natural-looking images. We draw inspiration from generative adversarial networks (GANs) where a generator network is trained to progressively generate more natural images that fool a discriminator model, in a min-max optimization scenario (Goodfellow et al., 2014). More specifically, we frame a classifier as the generator model in the GAN framework so that its Jacobians can progressively fool a discriminator model to interpret them as input images.

Another motivation lies in the high computational cost of the strongest defense to date, adversarial training. The cost on top of standard training is proportional to the number of steps its adversarial examples take to be crafted, requiring an additional backpropagation for each iteration. Especially with larger datasets, there is a need for less resource-intensive defense. In our proposed method (JARN), there is only one additional backpropagation through the classifier and the discriminator model on top of standard training. We share JARN in the following paragraphs and offer some theoretical analysis in § 3.1.

Jacobian Adversarially Regularized Networks Denoting input as $\mathbf{x} \in \mathbb{R}^{hwc}$ for $h \times w$-size images with c channels, one-hot label vector of k classes as $\mathbf{y} \in \mathbb{R}^k$, we express $f_{\text{cls}}(\mathbf{x}) \in \mathbb{R}^k$ as the prediction of the classifier (f_{cls}), parameterized by θ. The standard cross-entropy loss is

$$\mathcal{L}_{\text{cls}} = \mathbb{E}_{(\mathbf{x},\mathbf{y})}\left[-\mathbf{y}^\top \log f_{\text{cls}}(\mathbf{x})\right] \tag{5}$$

With gradient backpropagation to the input layer, through f_{cls} with respect to $\mathcal{L}_{\text{cls}}$, we can get the Jacobian matrix $J \in \mathbb{R}^{hwc}$ as:

$$J(\mathbf{x}) := \nabla_{\mathbf{x}}\mathcal{L}_{\text{cls}} = \begin{bmatrix} \dfrac{\partial \mathcal{L}_{\text{cls}}}{\partial \mathbf{x}_1} & \cdots & \dfrac{\partial \mathcal{L}_{\text{cls}}}{\partial \mathbf{x}_d} \end{bmatrix} \tag{6}$$

where $d = hwc$. The next part of JARN entails adversarial regularization of Jacobian matrices to induce resemblance with input images. Though the Jacobians of robust models are empirically observed to be similar to images, their distributions of pixel values do not visually match (Etmann et al., 2019). The discriminator model may easily distinguish between the Jacobian and natural images through this difference, resulting in the vanishing gradient (Arjovsky et al., 2017) for the classifier train on. To address this, an adaptor network (f_{apt}) is introduced to map the Jacobian into

the domain of input images. In our experiments, we use a single 1x1 convolutional layer with $tanh$ activation function to model f_{apt}, expressing its model parameters as ψ. With the J as the input of f_{apt}, we get the adapted Jacobian matrix $J' \in \mathbb{R}^{hwc}$,

$$J' = f_{\text{apt}}(J) \tag{7}$$

We can frame the classifier and adaptor networks as a generator $G(\mathbf{x}, \mathbf{y})$

$$G_{\theta,\psi}(\mathbf{x}, \mathbf{y}) = f_{\text{apt}}(\ \nabla_{\mathbf{x}} \mathcal{L}_{\text{cls}}(\mathbf{x}, \mathbf{y})\ ) \tag{8}$$

learning to model distribution of $p_{J'}$ that resembles $p_{\mathbf{x}}$.

We now denote a discriminator network, parameterized by ϕ, as f_{disc} that outputs a single scalar. $f_{\text{disc}}(\mathbf{x})$ represents the probability that $\mathbf{x}$ came from training images $p_{\mathbf{x}}$ rather than $p_{J'}$. To train $G_{\theta,\psi}$ to produce J' that f_{disc} perceive as natural images, we employ the following adversarial loss:

$$\begin{aligned}
\mathcal{L}_{\text{adv}} &= \mathbb{E}_{\mathbf{x}}[\log f_{\text{disc}}(\mathbf{x})] + \mathbb{E}_{J'}[\log(1 - f_{\text{disc}}(J'))] \\
&= \mathbb{E}_{\mathbf{x}}[\log f_{\text{disc}}(\mathbf{x})] + \mathbb{E}_{(\mathbf{x},\mathbf{y})}[\log(1 - f_{\text{disc}}(G_{\theta,\psi}(\mathbf{x})))] \\
&= \mathbb{E}_{\mathbf{x}}[\log f_{\text{disc}}(\mathbf{x})] + \mathbb{E}_{(\mathbf{x},\mathbf{y})}\ [\log(1 - f_{\text{disc}}(\ f_{\text{apt}}(\ \nabla_{\mathbf{x}} \mathcal{L}_{\text{cls}}(\mathbf{x}, \mathbf{y}))))]
\end{aligned} \tag{9}$$

Combining this regularization loss with the classification loss function $\mathcal{L}_{\text{cls}}$ in Equation (5), we can optimize through stochastic gradient descent to approximate the optimal parameters for the classifier f_{cls} as follows,

$$\theta^* = \arg\min_{\theta}(\mathcal{L}_{cls} + \lambda_{adv}\mathcal{L}_{adv}) \tag{10}$$

where λ_{adv} control how much Jacobian adversarial regularization term dominates the training.

Since the adaptor network (f_{apt}) is part of the generator G, its optimal parameters ψ^* can be found with minimization of the adversarial loss,

$$\psi^* = \arg\min_{\psi} \mathcal{L}_{adv} \tag{11}$$

On the other hand, the (f_{disc}) is optimized to maximize the adversarial loss term to distinguish Jacobian from input images correctly,

$$\phi^* = \arg\max_{\phi} \mathcal{L}_{adv} \tag{12}$$

Analogous to how generator from GANs learn to generate images from noise, we add $[-\varepsilon, -\varepsilon]$ uniformly distributed noise to input image pixels during JARN training phase. Figure 1 shows a summary of JARN training phase while Algorithm 1 details the corresponding pseudo-codes. In our experiments, we find that using JARN framework only on the last few epoch (25%) to train the classifier confers similar adversarial robustness compared training with JARN for the whole duration. This practice saves compute time and is used for the results reported in this paper.

3.1 Theoretical Analysis

Here, we study the link between JARN's adversarial regularization term with the notion of linearized robustness. Assuming a non-parameteric setting where the models have infinite capacity, we have the following theorem while optimizing G with the adversarial loss $\mathcal{L}_{adv}$.

Theorem 3.1. *The global minimum of $\mathcal{L}_{adv}$ is achieved when $G(\mathbf{x})$ maps $\mathbf{x}$ to itself, i.e., $G(\mathbf{x}) = \mathbf{x}$.*

Its proof is deferred to § A. If we assume Jacobian J of our classifier f_{cls} to be the direct output of G, then $J = G(\mathbf{x}) = \mathbf{x}$ at the global minimum of the adversarial objective.

In Etmann et al. (2019), it is shown that the linearized robustness of a model is loosely upper-bounded by the alignment between the Jacobian and the input image. More concretely, denoting Ψ^i as the logits value of class i in a classifier F, its linearized robustness ρ can be expressed as $\rho(\mathbf{x}) := \min_{j \neq i^*} \frac{\Psi^{i^*}(\mathbf{x}) - \Psi^j(\mathbf{x})}{\|\nabla_{\mathbf{x}}\Psi^{i^*}(\mathbf{x}) - \nabla_{\mathbf{x}}\Psi^j(\mathbf{x})\|}$. Here we quote the theorem from Etmann et al. (2019):

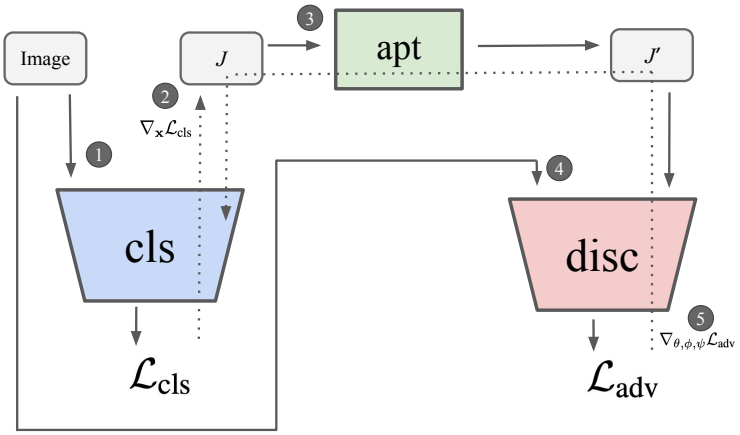

Figure 1: Training architecture of JARN.

Algorithm 1: Jacobian Adversarially Regularized Network

Input: Training data $\mathcal{D}_{\text{train}}$, Learning rates for classifier f_{cls}, adaptor f_{apt} and discriminator f_{disc}: (α, β, γ)
for *each training iteration* **do**
  Sample $(\mathbf{x}, \mathbf{y}) \sim \mathcal{D}_{\text{train}}$
  $\mathbf{x} \leftarrow \mathbf{x} + \xi, \quad \xi_i \sim \text{unif}[-\varepsilon, \varepsilon]$
  $\mathcal{L}_{\text{cls}} \leftarrow -\mathbf{y}^\top \log f_{\text{cls}}(\mathbf{x})$ ▷ (1) Compute classification cross-entropy loss
  $J \leftarrow \nabla_{\mathbf{x}} \mathcal{L}_{\text{cls}}$ ▷ (2) Compute Jacobian matrix
  $J' \leftarrow f_{\text{apt}}(J)$ ▷ (3) Adapt Jacobian to image domain
  $\mathcal{L}_{\text{adv}} \leftarrow \log f_{\text{disc}}(\mathbf{x}) + \log(1 - f_{\text{disc}}(J'))$ ▷ (4) Compute adversarial loss
  $\theta \leftarrow \theta - \alpha \nabla_\theta (\mathcal{L}_{cls} + \lambda_{adv} \mathcal{L}_{adv})$ ▷ (5a) Update the classifier f_{cls} to minimize $\mathcal{L}_{cls}$ and $\mathcal{L}_{adv}$
  $\psi \leftarrow \psi - \beta \nabla_\psi \mathcal{L}_{adv}$ ▷ (5b) Update the adaptor f_{apt} to minimize $\mathcal{L}_{adv}$
  $\phi \leftarrow \phi + \gamma \nabla_\phi \mathcal{L}_{adv}$ ▷ (5b) Update the adaptor f_{apt} to maximize $\mathcal{L}_{adv}$

Theorem 3.2 (Linearized Robustness Bound). *(Etmann et al., 2019) Defining $i^* = \arg\max_i \Psi^i$ and $j^* = \arg\max_{j \neq i^*} \Psi^j$ as top two prediction, we let the Jacobian with respect to the difference in top two logits be $g := \nabla_{\mathbf{x}}(\Psi^{i^*} - \Psi^{j^*})(\mathbf{x})$. Expressing alignment between the Jacobian with the input as $\alpha(\mathbf{x}) = \frac{|\langle \mathbf{x}, g \rangle|}{\|g\|}$, then*

$$\rho(\mathbf{x}) \leq \alpha(\mathbf{x}) + \frac{C}{\|g\|} \tag{13}$$

where C is a positive constant.

Combining with what we have in Theorem 3.1, assuming J to be close to g in a fixed constant term, the alignment term $\alpha(\mathbf{x})$ in Equation (13) is maximum when $\mathcal{L}_{\text{adv}}$ reaches its global minimum. Though this is not a strict upper bound and, to facilitate the training in JARN in practice, we use an adaptor network to transform the Jacobian, i.e., $J' = f_{\text{apt}}(J)$, our experiments show that model robustness can be improved with this adversarial regularization.

4 Experiments

We conduct experiments on three image datasets, MNIST, SVHN and CIFAR-10 to evaluate the adversarial robustness of models trained by JARN.

4.1 MNIST

Setup MNIST consists of 60k training and 10k test binary-colored images. We train a CNN, sequentially composed of 3 convolutional layers and 1 final softmax layer. All 3 convolutional layers have a stride of 5 while each layer has an increasing number of output channels (64-128-256).

For JARN, we use $\lambda_{\text{adv}} = 1$, a discriminator network of 2 CNN layers (64-128 output channels) and update it for every 10 f_{cls} training iterations. We evaluate trained models against adversarial examples with l_∞ perturbation $\varepsilon = 0.3$, crafted from FGSM and PGD (5 & 40 iterations). FGSM generates weaker adversarial examples with only one gradient step and is weaker than the iterative PGD method.

Results The CNN trained with JARN shows improved adversarial robustness from a standard model across the three types of adversarial examples (Table 1). In the MNIST experiments, we find that data augmentation with uniform noise to pixels alone provides no benefit in robustness from the baseline.

Table 1: MNIST accuracy (%) on adversarial and clean test samples.

Model	FGSM	PGD5	PGD40	Clean
Standard	76.5	0	0	98.7
Uniform Noise	77.5	0	0.02	98.7
JARN	**98.4**	**98.1**	**98.1**	98.8

4.2 SVHN

Setup SVHN is a 10-class house number image classification dataset with 73257 training and 26032 test images, each of size 32x32x3. We train the Wide-Resnet 32-10 model following hyper-parameters from (Madry et al., 2017)'s setup for their CIFAR-10 experiments. For JARN, we use $\lambda_{\text{adv}} = 5$, a discriminator network of 5 CNN layers (16-32-64-128-256 output channels) and update it for every 20 f_{cls} training iterations. We evaluate trained models against adversarial examples with ($\varepsilon = 8/255$), crafted from FGSM and 5, 10, 20-iteration PGD attack.

Results Similar to the findings in § 4.1, JARN advances the adversarial robustness of the classifier from the standard baseline against all four types of attacks. Interestingly, uniform noise image augmentation increases adversarial robustness from the baseline in the SVHN experiments, concurring with previous work that shows noise augmentation improves robustness (Ford et al., 2019).

Table 2: SVHN accuracy (%) on adversarial and clean test samples.

Model	FGSM	PGD5	PGD10	PGD20	Clean
Standard	64.4	26.0	5.47	1.96	94.7
Uniform Noise	65.0	42.6	18.4	9.21	95.3
JARN	**67.2**	**57.5**	**37.7**	**26.79**	94.9

4.3 CIFAR-10

Setup CIFAR-10 contains 32x32x3 colored images labeled as 10 classes, with 50k training and 10k test images. We train the Wide-Resnet 32-10 model using similar hyperparameters to (Madry et al., 2017) for our experiments. Following the settings from Madry et al. (2017), we compare with a strong adversarial training baseline (PGD-AT7) that involves training the model with adversarial examples generate with 7-iteration PGD attack. For JARN, we use $\lambda_{\text{adv}} = 1$, a discriminator network of 5 CNN layers (32-64-128-256-512 output channels) and update it for every 20 f_{cls} training iterations. We evaluate trained models against adversarial examples with ($\varepsilon = 8/255$), crafted from FGSM and PGD (5, 10 & 20 iterations). We also add in a fast gradient sign attack baseline (FGSM-AT1) that generates adversarial training examples with only 1 gradient step. Though FGSM-trained models are known to rely on obfuscated gradients to counter weak attacks, we augment it with JARN to study if there is additive robustness benefit against strong attacks.

Results Similar to results from the previous two datasets, the JARN classifier performs better than the standard baseline for all four types of adversarial examples. Compared to the model trained with uniform-noise augmentation, JARN performs closely in the weaker FGSM attack while being more robust against the two stronger PGD attacks. The strong PGD-AT7 baseline shows higher robustness against PGD attacks than the JARN model. When we train JARN together with 1-step adversarial

training (JARN-AT1), we find that the model's robustness exceeds that of strong PGD-AT7 baseline on all four adversarial attacks, suggesting JARN's gain in robustness is additive to that of AT.

Table 3: CIFAR-10 accuracy (%) on adversarial and clean test samples.

Model	FGSM	PGD5	PGD10	PGD20	Clean
Standard	13.4	0	0	0	95.0
Uniform Noise	67.4	44.6	19.7	7.48	94.0
FGSM-AT1	**94.5**	0.25	0.02	0.01	91.7
JARN	67.2	50.0	27.6	15.5	93.9
PGD-AT7	56.2	55.5	47.3	45.9	87.3
JARN-AT1	65.7	**60.1**	**51.8**	**46.7**	84.8

4.3.1 Generalization of Robustness

Adversarial training (AT) based defenses generally train the model on examples generated by perturbation of a fixed ε. Unlike AT, JARN by itself does not have ε as a training parameter. To study how JARN-AT1 robustness generalizes, we conduct PGD attacks of varying ε and strength (5, 10 and 20 iterations). We also include another PGD-AT7 baseline that was trained at a higher $\varepsilon = (12/255)$. JARN-AT1 shows higher robustness than the two PGD-AT7 baselines against attacks with higher ε values ($\leq 8/255$) across the three PGD attacks, as shown in Figure 2. We also observe that the PGD-AT7 variants outperform each other on attacks with ε values close to their training ε, suggesting that their robustness is more adapted to resist adversarial examples that they are trained on. This relates to findings by Tramèr & Boneh (2019) which shows that robustness from adversarial training is highest against the perturbation type that models are trained on.

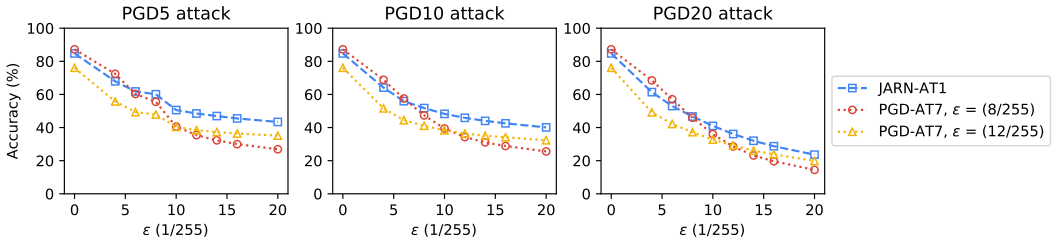

Figure 2: Generalization of model robustness to PGD attacks of different ε values.

4.3.2 Loss Landscape

We compute the classification loss value along the adversarial perturbation's direction and a random orthogonal direction to analyze the loss landscape of the models. From Figure 3, we see that the models trained by the standard and FGSM-AT method display loss surfaces that are jagged and non-linear. This explains why the FGSM-AT display modest accuracy at the weaker FGSM attacks but fail at attacks with more iterations, a phenomenon called obfuscated gradients (Carlini & Wagner, 2017; Uesato et al., 2018) where the initial gradient steps are still trapped within the locality of the input but eventually escape with more iterations. The JARN model displays a loss landscape that is less steep compared to the standard and FGSM-AT models, marked by the much lower (1 order of magnitude) loss value in Figure 3c. When JARN is combined with one iteration of adversarial training, the JARN-AT1 model is observed to have much smoother loss landscapes, similar that of the PGD-AT7 model, a strong baseline previously observed to be free of obfuscated gradients. This suggests that JARN and AT have additive benefits and JARN-AT1's adversarial robustness against strong PGD attacks is attributed by its resistance to obfuscated gradients.

4.3.3 Saliency of Jacobian

The Jacobian matrices of JARN model and PGD-AT are salient and visually resemble the images more than those from the standard model (Figure 4). Upon closer inspection, the Jacobian matrices of the PGD-AT model concentrate their values at small regions around the object of interest whereas those of the JARN model covers a larger proportion of the images. One explanation is that the JARN

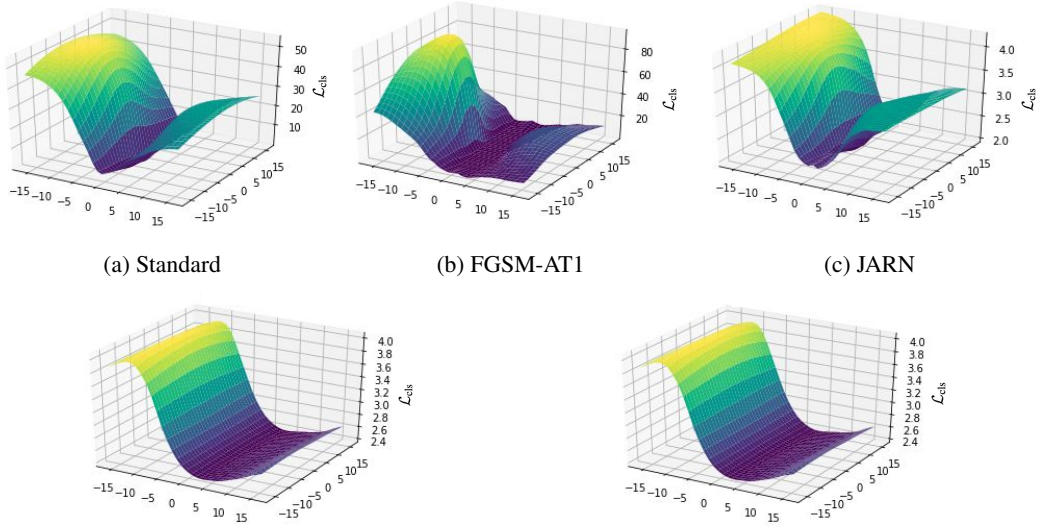

(a) Standard (b) FGSM-AT1 (c) JARN

(d) JARN-AT1 (e) PGD-AT7

Figure 3: Loss surfaces of models along the adversarial perturbation and a random direction.

model is trained to fool the discriminator network and hence generates Jacobian that contains details of input images to more closely resemble them.

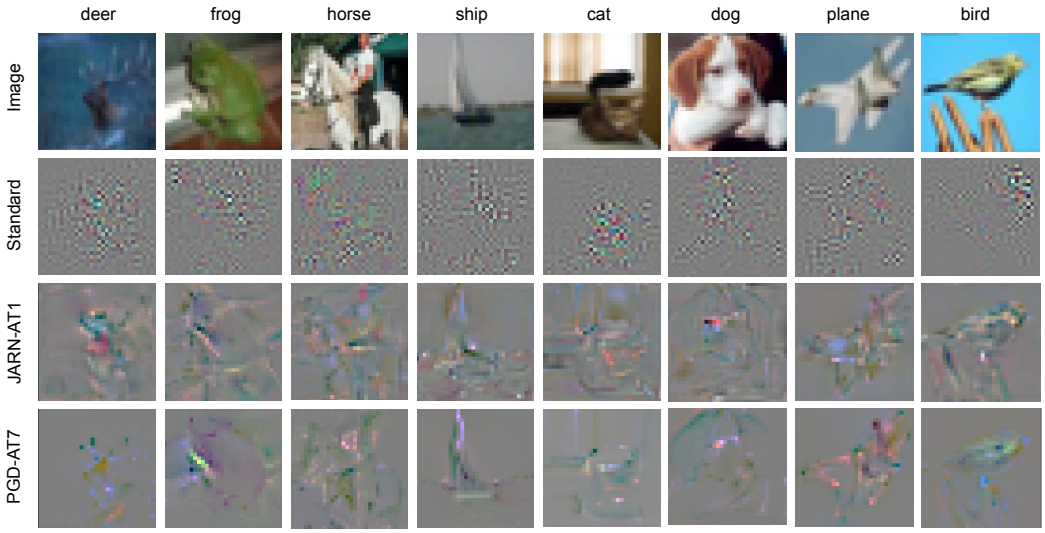

Figure 4: Jacobian matrices of CIFAR-10 models.

5 Conclusions

In this paper, we show that training classifiers to give more salient input Jacobian matrices that resemble images can advance their robustness against adversarial examples. We achieve this through an adversarial regularization framework (JARN) that train the model's Jacobians to fool a discriminator network into classifying them as images. Through our experiments in three image datasets, JARN boosts adversarial robustness of standard models and give competitive performance when added on to weak defenses like FGSM. Our findings open the viability of improving the saliency of Jacobian as a new avenue to boost adversarial robustness.

REFERENCES

Martin Arjovsky, Soumith Chintala, and Léon Bottou. Wasserstein gan. *arXiv preprint arXiv:1701.07875*, 2017.

Mariusz Bojarski, Davide Del Testa, Daniel Dworakowski, Bernhard Firner, Beat Flepp, Prasoon Goyal, Lawrence D Jackel, Mathew Monfort, Urs Muller, Jiakai Zhang, et al. End to end learning for self-driving cars. *arXiv preprint arXiv:1604.07316*, 2016.

Nicholas Carlini and David Wagner. Towards evaluating the robustness of neural networks. In *2017 IEEE Symposium on Security and Privacy (SP)*, pp. 39–57. IEEE, 2017.

Yunjey Choi, Minje Choi, Munyoung Kim, Jung-Woo Ha, Sunghun Kim, and Jaegul Choo. Stargan: Unified generative adversarial networks for multi-domain image-to-image translation. In *The IEEE Conference on Computer Vision and Pattern Recognition (CVPR)*, June 2018.

Francesco Croce and Matthias Hein. Minimally distorted adversarial examples with a fast adaptive boundary attack. *arXiv preprint arXiv:1907.02044*, 2019.

Bin Dai and David Wipf. Diagnosing and enhancing vae models. *arXiv preprint arXiv:1903.05789*, 2019.

Christian Etmann, Sebastian Lunz, Peter Maass, and Carola-Bibiane Schönlieb. On the connection between adversarial robustness and saliency map interpretability. *arXiv preprint arXiv:1905.04172*, 2019.

Nic Ford, Justin Gilmer, Nicolas Carlini, and Dogus Cubuk. Adversarial examples are a natural consequence of test error in noise. *arXiv preprint arXiv:1901.10513*, 2019.

Ian Goodfellow, Jean Pouget-Abadie, Mehdi Mirza, Bing Xu, David Warde-Farley, Sherjil Ozair, Aaron Courville, and Yoshua Bengio. Generative adversarial nets. In *Advances in neural information processing systems*, pp. 2672–2680, 2014.

Ian Goodfellow, Yoshua Bengio, Aaron Courville, and Yoshua Bengio. *Deep learning*, volume 1. MIT Press, 2016.

Sven Gowal, Krishnamurthy Dvijotham, Robert Stanforth, Rudy Bunel, Chongli Qin, Jonathan Uesato, Timothy Mann, and Pushmeet Kohli. On the effectiveness of interval bound propagation for training verifiably robust models. *arXiv preprint arXiv:1810.12715*, 2018.

Matthias Hein and Maksym Andriushchenko. Formal guarantees on the robustness of a classifier against adversarial manipulation. In *Advances in Neural Information Processing Systems*, pp. 2266–2276, 2017.

Daniel Jakubovitz and Raja Giryes. Improving dnn robustness to adversarial attacks using jacobian regularization. In *Proceedings of the European Conference on Computer Vision (ECCV)*, pp. 514–529, 2018.

Harini Kannan, Alexey Kurakin, and Ian Goodfellow. Adversarial logit pairing. *arXiv preprint arXiv:1803.06373*, 2018.

Yann LeCun, Yoshua Bengio, and Geoffrey Hinton. Deep learning. *nature*, 521(7553):436, 2015.

Aleksander Madry, Aleksandar Makelov, Ludwig Schmidt, Dimitris Tsipras, and Adrian Vladu. Towards deep learning models resistant to adversarial attacks. *arXiv preprint arXiv:1706.06083*, 2017.

Nicolas Papernot, Fartash Faghri, Nicholas Carlini, Ian Goodfellow, Reuben Feinman, Alexey Kurakin, Cihang Xie, Yash Sharma, Tom Brown, Aurko Roy, Alexander Matyasko, Vahid Behzadan, Karen Hambardzumyan, Zhishuai Zhang, Yi-Lin Juang, Zhi Li, Ryan Sheatsley, Abhibhav Garg, Jonathan Uesato, Willi Gierke, Yinpeng Dong, David Berthelot, Paul Hendricks, Jonas Rauber, and Rujun Long. Technical report on the cleverhans v2.1.0 adversarial examples library. *arXiv preprint arXiv:1610.00768*, 2018.

Chongli Qin, James Martens, Sven Gowal, Dilip Krishnan, Alhussein Fawzi, Soham De, Robert Stanforth, Pushmeet Kohli, et al. Adversarial robustness through local linearization. *arXiv preprint arXiv:1907.02610*, 2019.

Aditi Raghunathan, Jacob Steinhardt, and Percy S Liang. Semidefinite relaxations for certifying robustness to adversarial examples. In *Advances in Neural Information Processing Systems*, pp. 10877–10887, 2018.

Andrew Slavin Ross and Finale Doshi-Velez. Improving the adversarial robustness and interpretability of deep neural networks by regularizing their input gradients. In *Thirty-second AAAI conference on artificial intelligence*, 2018.

Ali Shafahi, Mahyar Najibi, Amin Ghiasi, Zheng Xu, John Dickerson, Christoph Studer, Larry S Davis, Gavin Taylor, and Tom Goldstein. Adversarial training for free! *arXiv preprint arXiv:1904.12843*, 2019.

Christian Szegedy, Wojciech Zaremba, Ilya Sutskever, Joan Bruna, Dumitru Erhan, Ian Goodfellow, and Rob Fergus. Intriguing properties of neural networks. *arXiv preprint arXiv:1312.6199*, 2013.

Florian Tramèr and Dan Boneh. Adversarial training and robustness for multiple perturbations. *arXiv preprint arXiv:1904.13000*, 2019.

Dimitris Tsipras, Shibani Santurkar, Logan Engstrom, Alexander Turner, and Aleksander Madry. Robustness may be at odds with accuracy. *arXiv preprint arXiv:1805.12152*, 2018.

Jonathan Uesato, Brendan O'Donoghue, Aaron van den Oord, and Pushmeet Kohli. Adversarial risk and the dangers of evaluating against weak attacks. *arXiv preprint arXiv:1802.05666*, 2018.

Eric Wong, Frank Schmidt, Jan Hendrik Metzen, and J Zico Kolter. Scaling provable adversarial defenses. In *Advances in Neural Information Processing Systems*, pp. 8400–8409, 2018.

Cihang Xie, Yuxin Wu, Laurens van der Maaten, Alan L Yuille, and Kaiming He. Feature denoising for improving adversarial robustness. In *Proceedings of the IEEE Conference on Computer Vision and Pattern Recognition*, pp. 501–509, 2019.

Haichao Zhang and Jianyu Wang. Defense against adversarial attacks using feature scattering-based adversarial training. *arXiv preprint arXiv:1907.10764*, 2019.

Hongyang Zhang, Yaodong Yu, Jiantao Jiao, Eric P Xing, Laurent El Ghaoui, and Michael I Jordan. Theoretically principled trade-off between robustness and accuracy. *arXiv preprint arXiv:1901.08573*, 2019.

A Proof of Theorem 3.1

Theorem A.1. *The global minimum of $\mathcal{L}_{adv}$ is achieved when $G(\mathbf{x})$ maps $\mathbf{x}$ to itself, i.e., $G(\mathbf{x}) = \mathbf{x}$.*

Proof. From (Goodfellow et al., 2014), for a fixed G, the optimal discriminator is

$$f^*_{\text{disc}}(\mathbf{x}) = \frac{p_{\text{data}}(\mathbf{x})}{p_{\text{data}}(\mathbf{x}) + p_G(\mathbf{x})} \tag{14}$$

We can include the optimal discriminator into Equation (9) to get

$$\begin{aligned}
\mathcal{L}_{\text{adv}}(G) &= \mathbb{E}_{\mathbf{x}\sim p_{\text{data}}}[\log f^*_{\text{disc}}(\mathbf{x})] + \mathbb{E}_{\mathbf{x}\sim p_{\text{data}}}[\log(1 - f^*_{\text{disc}}(G(\mathbf{x})))] \\
&= \mathbb{E}_{\mathbf{x}\sim p_{\text{data}}}[\log f^*_{\text{disc}}(\mathbf{x})] + \mathbb{E}_{\mathbf{x}\sim p_{\text{G}}}[\log(1 - f^*_{\text{disc}}(\mathbf{x}))] \\
&= \mathbb{E}_{\mathbf{x}\sim p_{\text{data}}}\left[\log \frac{p_{\text{data}}(\mathbf{x})}{p_{\text{data}}(\mathbf{x}) + p_G(\mathbf{x})}\right] + \mathbb{E}_{\mathbf{x}\sim p_{\text{G}}}\left[\log \frac{p_{\text{G}}(\mathbf{x})}{p_{\text{data}}(\mathbf{x}) + p_G(\mathbf{x})}\right] \\
&= \mathbb{E}_{\mathbf{x}\sim p_{\text{data}}}\left[\log \frac{p_{\text{data}}(\mathbf{x})}{\frac{1}{2}(p_{\text{data}}(\mathbf{x}) + p_G(\mathbf{x}))}\right] + \mathbb{E}_{\mathbf{x}\sim p_{\text{G}}}\left[\log \frac{p_{\text{G}}(\mathbf{x})}{\frac{1}{2}(p_{\text{data}}(\mathbf{x}) + p_G(\mathbf{x}))}\right] - 2\log 2 \\
&= KL\left(p_{\text{data}} \,\middle\|\, \frac{p_{\text{data}} + p_G}{2}\right) + KL\left(p_{\text{G}} \,\middle\|\, \frac{p_{\text{data}} + p_G}{2}\right) - \log 4 \\
&= 2 \cdot JS(p_{\text{data}}||p_{\text{G}}) - \log 4
\end{aligned} \tag{15}$$

where KL and JS are the Kullback-Leibler and Jensen-Shannon divergence respectively. Since the Jensen-Shannon divergence is always non-negative, $\mathcal{L}_{\text{adv}}(G)$ reaches its global minimum value of $-\log 4$ when $JS(p_{\text{data}}||p_{\text{G}}) = 0$. When $G(\mathbf{x}) = \mathbf{x}$, we get $p_{\text{data}} = p_{\text{G}}$ and consequently $JS(p_{\text{data}}||p_{\text{G}}) = 0$, thus completing the proof.

□